Available online at www.sciencedirect.com
ScienceDirect
Acta Materialia 56 (2008) 4890–4895
Acta MATERIALIA
www.elsevier.com/locate/actamat

Coercivity enhancement in boron-enriched stoichiometric REFeB melt-spun alloys

I. Betancourt [a,*], G. Cruz-Arcos [a], T. Schrefl [b], H.A. Davies [b]

[a] Departamento de Materiales Metálicos y Cerámicos, Instituto de Investigaciones en Materiales, Universidad Nacional Autónoma de México, 04510 México, D.F., Mexico
[b] Department of Engineering Materials, University of Sheffield, Sir Robert Hadfield Building, Mappin Street, Sheffield S1 3JD, UK

Received 6 March 2008; received in revised form 26 April 2008; accepted 4 June 2008
Available online 14 July 2008

Abstract

Considerable enhancement of magnetic properties was attained in initially stoichiometric nanophase $RE_{12}Fe_{82}B_6$ melt-spun alloys (RE = Nd, Nd + Pr) by means of an excess B content (10 at%) and additions of Zr and Co (2% and 7%, respectively). The intrinsic coercivity exhibited a marked improvement (with respect to the stoichiometric 6 at% B alloy), within the range 50–65%, with a maximum of 1161 ± 14 kA m^{-1} for the B-rich and Zr-containing alloy, together with an excellent combination of remanence and energy density values of 0.90 ± 0.01 T and 137 ± 4 kJ m^{-3}, respectively. Further Co addition led to a Curie temperature increase, while preserving high coercivity (1176 ± 31 kA m^{-1}) and useful energy densities (119 ± 4 kJ m^{-3}). Results were interpreted on the basis of alloy microstructural features and on variations of the intrinsic magnetic properties, supported by micromagnetic calculations.

Keywords: Nanocrystalline materials; Hard magnets; Coercivity; Micromagnetism

1. Introduction

Rare earth (RE)–iron–boron hard magnetic alloys have been the subject of intense study since their first announcement in 1984 [1,2] due to their outstanding combination of magnetic properties such as: high intrinsic coercivity $_iH_c$ (300–1500 kA m^{-1}, depending on RE content) and high maximum energy densities $(BH)_{max}$ (between 100 and 170 kJ m^{-3} for isotropic alloys) [3–5]. These alloys are the precursor materials for fabrication of permanent magnets, which can be used for a very wide range of applications: loudspeakers, uniform and non-uniform magnetic field sources, magnetic separation, magnetic bearings and couplings, levitation systems, actuators, sensors (anisotropic magnets), motors (dc, synchronous, stepping: isotropic magnets) and more recently, for biomedical devices, such as: cardiac valves, magnetic catheters, dental care and for "magnetotherapy" [6–9].

It is well established that the microstructure and magnetic properties of RE–Fe–B alloys are very sensitive to both the alloy composition and the processing parameters [3–6,9,10]. For melt-spun alloys, the stoichiometric composition (with RE content ~11.7 at%) results in isotropic alloys with a microstructure comprising uniaxial, randomly oriented crystallites and typical magnetic properties of $_iH_c$ between 700 and 800 kA m^{-1} and $(BH)_{max}$ within the range 110–170 kJ m^{-3} [3–5,9] (depending on the remanence J_r values, since $(BH)_{max}$ is approximately proportional to J_r^2 for materials with $\mu_{oi}H_c > J_r/2$ [11,12]). Reduction in the mean grain size d_g leads to an increasing degree of exchange interaction between magnetic moments on adjacent grains surface, which in turn leads to enhanced J_r values (well above the $0.5J_s$ limit expected for non-interacting, uniaxial, randomly oriented particles), though accompanied by reduced coercivities [3–5,9,13]. On the other hand, mixed rare-earth Nd–Pr–Fe–B based nanocomposite magnets are of interest because of the larger anisotropy constant K_1 for the $Pr_2Fe_{14}B$ phase than for its Nd counterpart (which results in higher $_iH_c$ values [3,9,14–

* Corresponding author. Tel.: +52 55 56224654; fax: +52 55 56161371.
E-mail address: israelb@correo.unam.mx (I. Betancourt).

1359-6454/$34.00 © 2008 Acta Materialia Inc. Published by Elsevier Ltd. All rights reserved.
doi:10.1016/j.actamat.2008.06.013

16]) and the absence of the spin reorientation phenomenon in $Pr_2Fe_{14}B$ [6,11–15], in addition to the potential economic benefit (i.e., lower cost) of employing didymium having Nd:Pr ratios that correspond to those that occur naturally in rare-earth ores (typically 3–4:1) [17]. In the present work, we report and discuss the effects of excess B and of Zr–Co additions on the magnetic properties of initially stoichiometric, isotropic melt-spun (NdPr)–Fe–B alloys.

2. Experimental details

Initial alloy ingots having compositions $Nd_2Fe_{82}B_6$, $RE_{12}Fe_{82}B_6$, $RE_{12}Fe_{78}B_{10}$, $RE_{12}Fe_{76}Zr_2B_{10}$ and $RE_{12}(Fe_{0.9}Co_{0.1})_{76}Zr_2B_{10}$ ($RE = Nd_{0.75}Pr_{0.25}$), were prepared using commercial-grade materials by arc-melting the constituents in a Ti-gettered, high-purity Ar atmosphere. Nanocrystalline alloy samples were obtained by a devitrification annealing (10 min at 700 °C, with ribbon samples sealed in a silica tube under argon) of initially fully amorphous alloy ribbons produced by chill block melt spinning using a roll speed of 30 m s^{-1}. The microstructure and d_g for selected ribbon samples were monitored by X-ray diffractometry (Bruker Advance D8 with monochromatic Cu-Kα radiation) and by transmission electron microscopy (Jeol 1200 TEM, with thin foils prepared by ion-beam thinning). The magnetic properties J_r, $_iH_c$ and $(BH)_{max}$ (computed from the B–H loop) were determined on at least 8 different samples with variable dimensions: 5–10 mm length and 20–25 μm thick, by using an Oxford Vibrating Sample Magnetometer with a maximum field of 5 T. Demagnetization field corrections were performed for M–H loops with demagnetizing factors between 0.000090 and 0.000014 corresponding to aspect ratios between 200 and 500 [18]. The reported value for magnetic properties was determined as an average, and the corresponding standard deviations were associated to the error intervals. The Curie temperature was estimated by means of magnetic thermogravimetric analysis (MTGA) with an applied magnetic field of 0.20 T. Micromagnetic simulations were performed by using time integration of the Landau–Lifshitz–Gilbert equation together with a hybrid FEM/BEM method [19] on realistic alloy models in the form of cubic structures of dimensions $100 \times 100 \times 100$ nm^3 and comprising 216 irregular grains in intimate contact, with the following intrinsic magnetic properties: $J_s^{Nd} = 1.61$ T, crystalline anisotropy $K_1^{Nd} = 4.3 \times 10^6$ J m^{-3} and exchange constant $A^{Nd} = 7.7 \times 10^{-12}$ J m^{-1} for the $Nd_2Fe_{14}B$ phase; and $J_s^{Pr} = 1.56$ T, $K_1^{Pr} = 5.6 \times 10^6$ J m^{-3} and $A^{Pr} = 12 \times 10^{-12}$ J m^{-1} for the $Pr_2Fe_{14}B$ phase [12].

3. Results

X-ray diffractograms for $Nd_{12}Fe_{82}B_6$, $RE_{12}Fe_{78}B_{10}$ and $RE_{12}(Fe_{0.9}Co_{0.1})_{76}Zr_2B_{10}$ alloys are shown in Fig. 1. All the peaks present correspond to the tetragonal $RE_2Fe_{14}B$ phase, as is expected for their stoichiometric 12 at% RE content. The same peak distribution was observed for the $RE_{12}Fe_{82}B_6$ and $RE_{12}Fe_{76}Zr_2B_{10}$ alloy samples (not shown). The mean grain sizes d_g for the complete alloy series, determined by means of the Scherrer formula for at least ten different peaks, are displayed in Table 1. A grain size refinement was observed after Pr addition (from 49 ± 7 nm to 35 ± 3 nm), followed by a general d_g coarsening for the B-enriched alloys (with the exception of the $RE_{12}Fe_{76}Zr_2B_{10}$ alloy, which in fact exhibits the smallest d_g throughout the alloy series). TEM micrographs of selected samples corresponding to $Nd_{12}Fe_{82}B_6$ and to the B-enriched $RE_{12}Fe_{78}B_{10}$ alloy ribbons are shown in Fig. 2. For the $Nd_{12}Fe_{82}B_6$ reference alloy sample (Fig. 2a) an isotropic distribution of 2/14/1 grains is manifested, with an approximate d_g value of 46 ± 4 nm, which is in good agreement with the grain size determined by XRD results (Table 1). Similar characteristics are displayed for the $RE_{12}Fe_{78}B_{10}$ alloy ribbon (Fig. 2b), with the presence of few fine precipitates (of about 10–20 nm) interspersed around the hard $RE_2Fe_{14}B$ grains as additional feature. These small crystallites would be afforded by the excess of B (probably as an iron boride [20]), thus forming a minor secondary phase with a volume fraction lower than the 5% minimum for XRD detection.

Magnetic TGA traces for the complete alloy series are displayed in Fig. 3. For the base $Nd_{12}Fe_{82}B_6$ ribbon sample, T_c was 310 °C, in accord with the reported value of 312 °C for the 2/14/1 phase [21]. A slight decrement of T_c (down to 307 °C) was recorded upon 3 at% Pr substitution, which can be associated with the lower T_c for the $Pr_2Fe_{12}B$ phase than for its $Nd_2Fe_{14}B$ counterpart [21]. The same T_c value was observed for the boron-enriched $RE_{12}Fe_{78}B_{10}$ alloy, which would imply that the excess of B is segregating outside the 2/14/1 grains. A significant reduction is exhibited for the Zr doped ribbon sample (282 °C) due to the deleterious effect

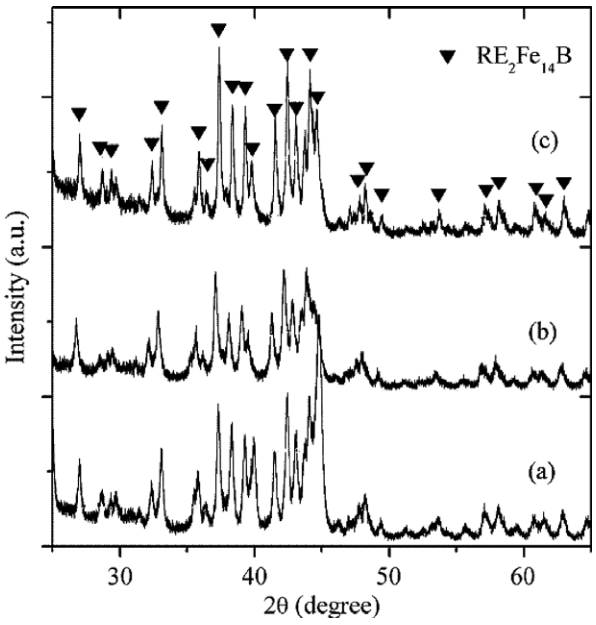

Fig. 1. X-ray diffractograms for: (a) $Nd_{12}Fe_{82}B_6$, (b) $RE_{12}Fe_{78}B_{10}$, and (c) $RE_{12}(Fe_{0.9}Co_{0.1})_{76}Zr_2B_{10}$ alloys.